HTML ABSTRACT * LINKS

Mechanical elasticity of single and double clamped silicon nanobeams fabricated by the vapor-liquid-solid method

A. San Paulo,[a] J. Bokor, and R. T. Howe
Department of Electrical Engineering and Computer Sciences, University of California, Berkeley, California 94720

R. He and P. Yang
Department of Chemistry, University of California, Berkeley, California 94720

D. Gao, C. Carraro, and R. Maboudian
Department of Chemical Engineering, University of California, Berkeley, California 94720

(Received 21 April 2005; accepted 18 June 2005; published online 29 July 2005)

Atomic force microscopy has been used to characterize the mechanical elasticity of Si nanowires synthesized by the vapor-liquid-solid method. The nanowires are horizontally grown between the two facing Si(111) sidewalls of microtrenches prefabricated on a Si(110) substrate, resulting in suspended single and double clamped nanowire-in-trench structures. The deflection of the nanowires is induced and measured by the controlled application of normal forces with the microscope tip. The observed reversibility of the nanowire deflections and the agreement between the measured deflection profiles and the theoretical behavior of single and double clamped elastic beams demonstrate the overall beamlike mechanical behavior and the mechanical rigidity of the clamping ends of the nanowire-in-trench structures. These results demonstrate the potential of the nanowire-in-trench fabrication approach for the integration of VLS grown nanostructures into functional nanomechanical devices. © *2005 American Institute of Physics*.
[DOI: 10.1063/1.2008364]

Semiconductor nanowires have unique properties for their application as building blocks in nanoelectromechanical systems (NEMS).[1–4] The vapor-solid-liquid (VLS) method for the growth of Si nanowires[5–8] is one of the most promising techniques for the development of such applications because of its control over the nanowire properties and its compatibility with standard microfabrication technology. So far, VLS-grown Si nanowires have been mostly applied in nanoelectronic devices.[4,9] Nanomechanical applications of these materials such as ultrasensitive force[3] or mass[10] sensing, or the study of the quantum limits of nanomechanical resonators,[11] remain largely unexplored. Such applications demand the availability of nanofabrication approaches that allow the mechanical integration of the VLS-synthesized nanostructures into functional NEMS.

The VLS method leads to the epitaxial growth of the nanowires from small catalyst particles deposited on a Si{111} substrate.[8,12–14] Thus, a mechanically rigid anchor can be expected at the base of the nanowire. If the nanowires are horizontally grown in microtrenches, they can form bridges that connect the two opposing vertical sidewalls.[14] In this case, scanning electron microscopy (SEM) images suggest that when a growing nanowire impinges on the opposite sidewall, it also makes a mechanically rigid connection. However, the mechanical rigidity of the clamping ends of nanowires grown in microtrenches cannot be properly determined from SEM images alone. On the other hand, atomic force microscopy (AFM) has been demonstrated as a powerful and versatile tool for the characterization of mechanical properties of different nanowirelike systems.[15–19] In this letter we employ the VLS method to grow suspended Si nanowires between the facing (111) sidewalls of microtrenches prefabricated on a Si(110) substrate, and we investigate the mechanical behavior of the resulting single and double clamped nanowire-in-trench structures by contact-mode AFM.

Single and double clamped Si nanowires are grown in 6-μm-deep and 1–12-μm-wide microtrenches fabricated by conventional photolithography on Si(110) substrates [Fig. 1(a)]. A proper alignment of the pattern ensures that the {111} planes are exposed in the sidewalls of the trenches.[14] After the fabrication of the trenches, Au nanoparticles are dis-

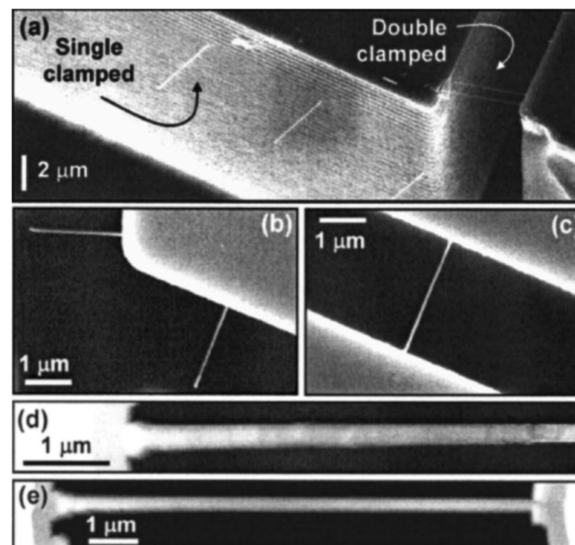

FIG. 1. (a) SEM image of nanowire-in-trench structures. SEM images of (b) single and (c) double clamped Si nanowires grown at the edge of the sidewalls; AFM images of (d) single and (e) double clamped Si nanowires.

[a]Electronic mail: alvaro@eecs.berkeley.edu

 © 2005 American Institute of Physics
Downloaded 09 Nov 2007 to 128.32.205.190. Redistribution subject to AIP license or copyright, see http://apl.aip.org/apl/copyright.jsp

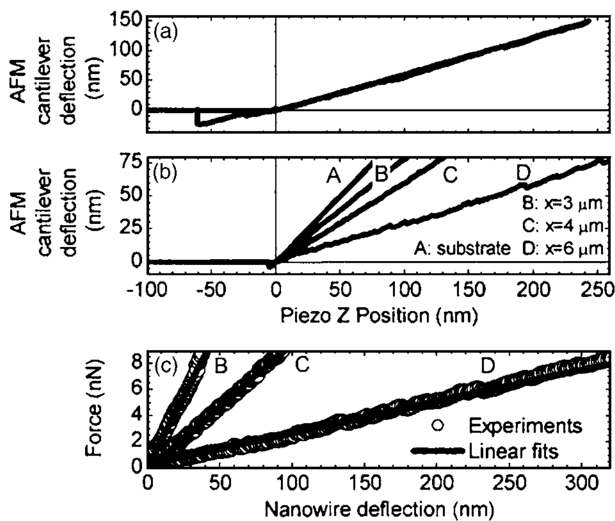

FIG. 2. (a) AFM cantilever deflection vs piezo position plot (approach and retract) obtained on a single clamped nanowire at 4 μm from its base. (b) Cantilever deflection plots (approach only) on the substrate and on the nanowire at 3, 4, and 5 μm from its base. (c) Force vs nanowire deflection curves obtained from the cantilever deflection curves.

persed on the substrate to serve as local catalysts centers for the VLS reaction. $SiCl_4$ is used as the precursor gas for the growth of the nanowires in a chemical vapor deposition system at 800–850 °C.[12] The nanowires typically range from a few tens to a few hundreds of nanometers in diameter, depending on the diameter of the Au catalyst particles used. Au particles absorbed very close to the edges of the vertical sidewalls produce suspended nanowires at optimum locations for AFM measurements [Figs. 1(b) and 1(c)]. A standard contact-mode AFM is used for the mechanical characterization of the nanowires. For the precise control of the applied normal force, Si_3N_4 cantilevers with a low spring constant of $k_c=0.12$ N/m (calibrated by the corrected thermal method[20]) are used. The cantilever orientation and the fast scan direction of the tip are, respectively, perpendicular and parallel to the nanowires. Scan speeds are in the 1–10 μm/s range. Two different measurements of the nanowire deflection d_{nw} are performed. First, the deflection at a fixed position x along the nanowire length is obtained as a function of the applied force. Second, the deflection profile of the nanowire is measured by scanning the AFM tip along its length at a constant applied force. The particular experiments reported here are performed on the single and double clamped nanowires shown in the AFM topography images of Figs. 1(d) and 1(e). The average diameters of these nanowires are 120 and 190 nm and their lengths are 8 and 12 μm, respectively, as measured by high-resolution SEM (not shown). Equivalent results were obtained on several nanowires with diameters ranging from 60 to 200 nm, and lengths ranging from 1 to 12 μm.

Figure 2 shows the deflection measurements on a single clamped nanowire as a function of the force applied at different positions along its length. Figure 2(a) is a standard AFM cantilever deflection d_c vs the vertical piezo position plot obtained on top of the nanowire, 4 μm from its base. The slope of the curve for positive deflections takes an average value of 0.63, instead of the value of 1 that would have been obtained on a rigid substrate. This result is a consequence of the nanowire deflection as the applied force is increased. On the other hand, the absence of a significant hysteresis between the approach and retract portions of the curve for positive deflections implies the reversibility of the nanowire deflection and the absence of detectable plastic deformations in the structure. The approach portions of several curves of the cantilever deflection versus the vertical piezo position, obtained at different positions along the nanowire length, are plotted together for comparison in Fig. 2(b). Curve A is obtained on the substrate as a reference, and it shows the expected slope of 1. Curves B, C, and D are obtained at $x=3$, 4, and 6 μm from the base of the nanowire. These curves behave linearly regardless of x, but their slope increases as x decreases, indicating that the effective stiffness of the nanowire increases as the distance to the base decreases.

The nanowire stiffness can be determined by plotting its deflection versus the applied force. The nanowire deflection can be calculated by subtracting the cantilever deflection curves B, C, and D obtained on the nanowire from the curve A obtained on the substrate. The force is calculated by using $F_c=k_c d_c$. The results, shown in Fig. 2(c), show linear nanowire deflections of up to several hundreds of nanometers under applied forces of a few nanonewtons. Linear fits to these curves yield nanowire spring constants k_{nw} of 0.22, 0.10, and 0.03 N/m at 3, 4, and 6 μm from the nanowire base, respectively. These numbers are consistent with the expected behavior of a single clamped elastic beam, in which the effective spring constant k as a function of the distance to the base end x is given by $k(x)=3EI/x^3$, where E is the Young's modulus, I is the moment of inertia, and the product EI is referred to as the bending stiffness of the beam. Calculating $k_{nw}x^3/3$ for each of the obtained values of k_{nw} at the corresponding distance x results in a value for the bending stiffness $EI=1.9$ N nm^2 with a standard deviation of only 8%. Assuming a uniform cylindrical cross section of the nanowire ($I=\pi r^4/4$) and using the experimental value of the nanowire diameter allows an estimate of $E=186$ GPa, which agrees well with the bulk value of 169 GPa for Si(111). The small discrepancy between the estimated and bulk values of E is mainly attributed to experimental error in the nanowire diameter.

Figure 3 shows the results of the force-deflection measurements obtained on a double clamped nanowire. Again, a standard cantilever deflection curve with a slope smaller than 1 (0.70 in this case) indicates that as the force applied by tip increases, the deflection of the nanowire increases [Fig. 3(a)]. Also, the overlapping of the approach and retraction curves implies the absence of detectable plastic deformations. However, this case shows a slightly nonlinear behavior of the nanowire deflection versus the applied force. Figure 3(c) displays the force versus nanowire deflection obtained from the cantilever deflection curves acquired on the substrate (A) and on the center of the nanowire (B), which are shown in Fig. 3(b). The nanowire deflection is linear below approximately 50 nm. Above this value, the plot is best fitted by including a cubic term in the force equation $F=k_l d_{nw} + k_3 d_{nw}^3$, and the fitting results in $k_l=0.45$ N/m and $k_2=2 \times 10^{-23}$ N/m^3. This is the expected behavior for a double clamped beam under sufficiently large deflections, where the stretching of the beam as it bends adds a cubic term to the force equation.

Nanowire deflection profiles under the application of a constant normal force are measured by the acquisition of two images of the nanowires. The first image is obtained with a

Downloaded 09 Nov 2007 to 128.32.205.190. Redistribution subject to AIP license or copyright, see http://apl.aip.org/apl/copyright.jsp

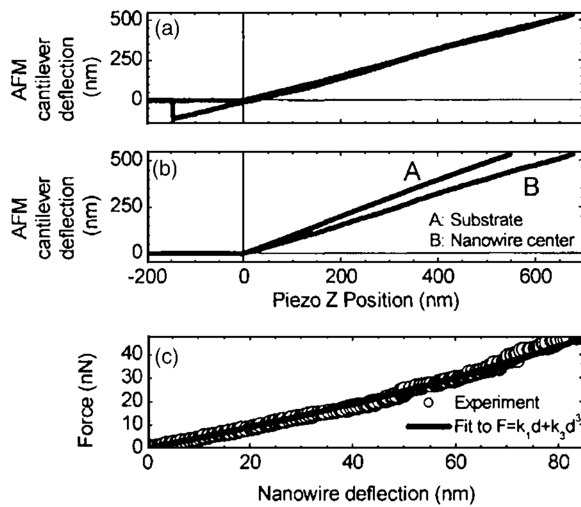

FIG. 3. (a) AFM cantilever deflection vs piezo position plot (approach and retract) on a double clamped nanowire at its center. (b) Cantilever deflection plots (approach only) on the substrate and on the nanowire center. (c) Force vs nanowire deflection curves obtained from the cantilever deflection curves.

set-point force equal to zero, while the second one is obtained with a particular nonzero set-point force. Subtracting the second image from the first one produces an image of the nanowire deflection under the force applied in the second image. The nanowire deflection profile is then extracted from a cross section of the resulting image along the longitudinal axis of the nanowire. Figure 4(a) shows three deflection profiles of the single clamped nanowire, corresponding to applied forces of 2.2, 6.6, and 11 nN. The profiles are shown for distances up to 3 μm from the base end. At larger distances, lateral deflections of the nanowire prevent a stable scanning of the tip. Each of the profiles shown in Fig. 4(a) fits well to the equation for the deflection of a single clamped beam under the application of a point load F at a position x along its length, which follows a cubic power law given by $d(x)=Fx^3/3EI$. The bending stiffness EI is used as the fitting parameter, and consistently with the previous force-deflection measurements, we obtain an average value of EI $=1.8$ N nm^2 with a standard deviation of only 1%. Figure 4(b) shows the deflection profiles obtained along the whole

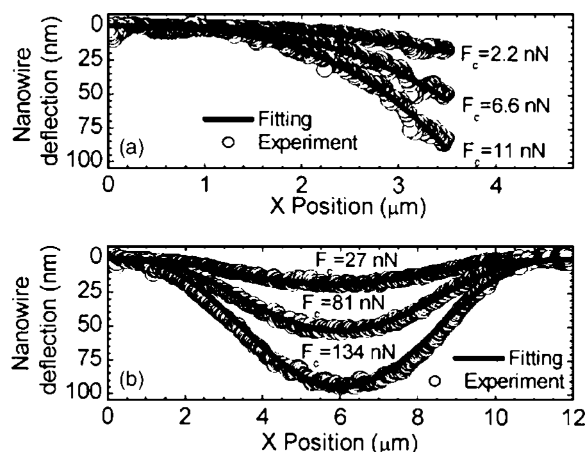

FIG. 4. Deflection profiles of (a) a single and (b) a double clamped nanowire under the application of different normal forces. The experimental profiles (dots) fit remarkably well to the theoretical profiles (lines) of single and double clamped elastic beams.

length l of a double clamped nanowire with applied forces of 27, 81, and 134 nN. Neglecting nonlinear contributions, the deflection of a double-clamped beam at position x is given by $d=Fl^3/3EI/(x/l)^3/(x/l-1)^3$. Each profile in Fig. 4(b) fits this expression remarkably well, with EI as the fitting parameter. An average value of $EI=13.3$ N nm^2 with a standard deviation of only 2% is obtained. Also, in this case, a reasonable value of $E=207$ GPa is deduced by assuming a cylindrical section of the nanowire and using the measured average diameter.

In conclusion, we have applied contact-mode AFM for the mechanical characterization of nanowire-in-trench structures grown by the VLS method. The agreement between the nanowire deflection measurements and the theoretical behavior of single and double clamped elastic beams demonstrate the overall elastic beamlike behavior and the rigidity of the clamping points of the nanowire-in-trench structures. Other "bottom-up" fabrication approaches[3,16] require nonideal anchoring using adhesion forces or metal/oxide deposition, introducing interfacial mechanical instabilities and additional energy dissipation mechanisms in resonant systems. In contrast, this nanowire-in-trench strategy produces self-assembled nanobeams solidly connected to prefabricated microstructures, allowing the direct integration of chemically synthesized nanoscale building blocks into functional NEMS.

This work is supported by the NSF (Grants No. DMI-0304209 and No. EEC-0425914) and DARPA (Project No. N6600-01-1-8967). A. S. P. acknowledges support from DURSI. P. Y. has a consulting relationship with Nanosys. Inc., who might benefit from the eventual commercialization of this research.

[1]H. G. Craighead, Science **290**, 1532 (2000).
[2]X. M. H. Huang, C. A. Zorman, M. Mehregany, and M. L. Roukes, Nature (London) **421**, 496 (2003).
[3]V. Sazonova, Y. Yaish, H. Üstünel, D. Roundy, T. A. Arias, and P. L. McEuen, Nature (London) **431**, 284 (2004).
[4]F. Patolsky, G. Zheng, O. Hayden, M. Lakadamyali, X. Zhuang, C. M. Lieber, Proc. Natl. Acad. Sci. U.S.A. **101**, 14017 (2004).
[5]R. S. Wagner and W. C. Ellis, Appl. Phys. Lett. **4**, 89 (1964).
[6]J. Westwater, D. P. Gosain, S. Tomiya, and S. Usui, J. Vac. Sci. Technol. B **15**, 554 (1997).
[7]A. M. Morales and C. M. Lieber, Science **279**, 208 (1998).
[8]Y. Wu and P. Yang, J. Am. Chem. Soc. **123**, 3165 (2001).
[9]D. Li, Y. Wu, P. Kim, L. Shi, P. Yang, and A. Majumdar, Appl. Phys. Lett. **83**, 2934 (2003).
[10]K. L. Ekinci, X. M. Huang, and M. L. Roukes, Appl. Phys. Lett. **84**, 4469 (2004).
[11]M. D. LaHaye, O. Buu, B. Camarota, and K. C. Schwab, Science **304**, 74 (2004).
[12]A. I. Hochbaum, R. Fan, R. He, and P. Yang, Nano Lett. **5**, 457 (2005).
[13]M. S. Islam, S. Sharma, T. I. Kamins, and R. S. Williams, Nanotechnology **15**, L5 (2004).
[14]R. He, D. Gao, R. Fan, A. I. Hochbaum, C. Carraro, R. Maboudian, and P. Yang, Adv. Mater. (to be published).
[15]E. W. Wong, P. E. Sheehan, and C. M. Lieber, Science **277**, 1971 (1997).
[16]J.-P. Salvetat, G. A. D. Briggs, J.-M. Bonard, R. R. Bacsa, A. J. Kulik, T. Stöckli, N. A. Burnham, and L. Forró, Phys. Rev. Lett. **82**, 944 (1999).
[17]T. W. Tombler, C. Zhou, L. Alexseyev, J. Kong, H. Dai, L. Liu, C. S. Jayanthi, M. Tang, and S. Wu, Nature (London) **405**, 769 (2000).
[18]J. Cao, Q. Wang, and H. Dai, Phys. Rev. Lett. **90**, 157601 (2003).
[19]E. D. Minot, Y. Yaish, V. Sazonova, J.-Y. Park, M. Brink, and P. L. McEuen, Phys. Rev. Lett. **90**, 156401 (2003).
[20]D. A. Walters, J. P. Cleveland, N. H. Thomson, P. K. Hansma, M. A. Wendman, G. Gurley, and V. Elings, Rev. Sci. Instrum. **67**, 3583 (1996).

Downloaded 09 Nov 2007 to 128.32.205.190. Redistribution subject to AIP license or copyright, see http://apl.aip.org/apl/copyright.jsp